A Method to Determine Nonhydrostatic Effects within Subdomains in a Mesoscale Model

J. L. SONG, R. A. PIELKE, M. SEGAL, R. W. ARRITT AND R. C. KESSLER

Department of Atmospheric Science, Colorado State University, Fort Collins, CO 80523

(Manuscript received 2 July 1984, in final form 9 April 1985)

ABSTRACT

The exact solution of the nonhydrostatic pressure residual (total pressure perturbation minus hydrostatic pressure perturbation) in Defant's linear model is derived. The quasi-nonhydrostatic residual, introduced by Pielke, and the pressure-correction term by Orlanski are compared with the exact residual for varying physical situations. It is found that, within the linear framework, nonhydrostatic effects generally become relatively more important when the environmental stability is near the neutral state and/or the associated horizontal length scale is several kilometers or smaller. The residual components associated with buoyancy and horizontal momentum are the two important physical mechanisms contributing to the generation of nonhydrostatic effects. In a near-neutral environment, a pressure residual must include the horizontal momentum nonhydrostatic residual in order to approximate more accurately the nonhydrostatic effects, while in a sufficiently stable environment the total pressure tends to behave hydrostatically, although the nonhydrostatic effect which does occur is associated with the nonhydrostatic buoyancy term.

The residual approach has the advantage in a numerical model in that it need only be applied in a subdomain of a model where vertical accelerations are important, while the more economical hydrostatic equation for pressure can be used elsewhere.

1. Introduction

Defant's linear model for local thermally-induced circulations (Defant, 1951) is utilized to analyze the magnitude of nonhydrostatic effects in a linear model and to investigate the accuracy of several methods for the potential incorporation of these effects into mesoscale numerical models. Martin and Pielke (1983) used the Defant model, together with a nonlinear analogue, to investigate the adequacy of the hydrostatic assumption for sea breeze circulations over a flat surface. Among their results, they showed that in a linear framework the hydrostatic assumption is accurate for scales of heating of only a few kilometers, provided the environment is stable and the subgrid-scale heat diffusion is not strong. When nonlinear advections were added, the scale of the response (i.e., the scale of the sea breeze circulation) tends to become smaller than the scale of the surface forcing. Thus, the scale-dependence of the hydrostatic assumption derived from a linear framework may not be valid in a nonlinear system.

It is of practical interest to know quantitatively how the nonhydrostatic terms in a primitive equation model would behave under varying physical conditions. A detailed study of this type should, of course, include advective effects, and perhaps also consider the situations when nonlinear forcing exists (as suggested in Martin and Pielke, 1983; and Orlanski, 1981). The Defant model is certainly insufficient for such a complete analysis. Pielke (1984) indicates some shortcomings of the Defant model, namely that: 1) the subgrid-scale turbulent exchange coefficients are independent of time and space, 2) the advection of temperature and velocity are ignored, 3) the environmental stability is considered a constant, 4) the surface temperature perturbation is prescribed, and 5) no nonlinear interactions are permitted among the dependent variables.

However, the Defant model does permit an evaluation of several of the important forcings (in a linear framework) in a thermally forced atmospheric system. Since the use of the Defant model provides mathematically exact solutions, such a linear analytic model provides investigators with the ability to explore the significance of many important processes without the complication of computational errors. Besides, once the linear processes are well understood, the important nonlinear processes can be added later on and studied in a focused and more clear manner.

There are several procedures to evaluate computationally nonhydrostatic effects in the atmosphere. For example, the total pressure perturbation can be solved directly from the ideal gas law in a nonhydrostatic, fully compressible model (Klemp and Wilhelmson, 1978; Cotton and Tripoli, 1978; Tapp and White, 1976; etc.), or, it may be solved using a Poisson-type of equation in an anelastic model (Ogura and Charney, 1961; Neumann and Mahrer, 1971; Schlesinger, 1978; etc.). For a mesoscale, incompressible model, Pielke (1972) derived a residual method which utilizes a Poisson-

type of equation, but for the nonhydrostatic residuals only (the "residual" for any physical variable is defined in this study by subtracting the value of that variable when obtained assuming pressure varies hydrostatically from the value when no hydrostatic assumption is made). The computational advantage of such a residual method over the complete Poisson equation approach as reported in Pielke (1984), is that it can be evaluated for only a subregion of a model, while in the remainder of the domain, where the vertical accelerations are less, the more economical hydrostatic equation for pressure can be applied. As a result of the boundary condition for the residual in the subdomain (i.e., the residual equals zero), the residual method is easier to implement computationally than the complete Poisson equation. The residual method can also be applied at selected periods during an integration (i.e., when nonhydrostatic effects become large), rather than the entire integration period. Orlanski (1981) suggested a simple modification in hydrostatic model equations, in order to account to some extent for nonhydrostatic effects (i.e., his quasi-hydrostatic approximation).

In the present study, the Pielke (1972) and the Orlanski (1981) approaches will be applied in the Defant model in order to examine the accuracy and applicability of the residual solution techniques suggested in Pielke (1972) and Orlanski (1981), as compared with the exact solution.

The factors which are considered significant in affecting both the relative importance of nonhydrostatic effects and the applicability of the residual technique (in a linear framework) are: horizontal length scale, large scale stability, subgrid-scale heat diffusion, strength of surface heating, and friction. Each of these physical parameters will be discussed with respect to its influence on the nonhydrostatic pressure. In Section 2, the exact solution of the nonhydrostatic residual will first be derived, which will then be simplified such that it can be applied using only information from a hydrostatic model. The solutions will then be tested under different physical conditions in Section 3.

These tests of the relative magnitudes of nonhydrostatic effects are similar to those performed in Martin and Pielke (1983). However, this study is distinct from that study in that we derive a mathematically exact solution of the nonhydrostatic pressure residual, while in that study the residual was obtained by merely differencing the nonhydrostatic and hydrostatic solutions of the Defant governing equations. Furthermore, once the exact residual is derived, simplifications can be made upon it to derive a prognostic method such that the method can be of practical value in a mesoscale numerical model.

In Section 4, the exact residual is compared with three other residual approximations, two of which correspond to the approaches introduced in Pielke (1972) and Orlanski (1981). The important physical mechanisms which contribute to the generation of nonhydrostatic effects are examined through the comparisons. Finally, the conclusion of this study is given in Section 5.

2. The nonhydrostatic residuals

The governing equations of the two-dimensional Defant model (as used in Pielke, 1984; and Martin and Pielke, 1983) are:

$$\frac{\partial u}{\partial t} = -\alpha_0 \frac{\partial p}{\partial x} + fv - \sigma_x u \tag{1}$$

$$\frac{\partial v}{\partial t} = -fu - \sigma_x v \tag{2}$$

$$\lambda \frac{\partial w}{\partial t} = \theta \frac{g}{\theta_0} - \alpha_0 \frac{\partial p}{\partial z} - \lambda \sigma_z w \tag{3}$$

$$\frac{\partial u}{\partial x} + \frac{\partial w}{\partial z} = 0 \tag{4}$$

$$\frac{\partial \theta}{\partial t} = -w \frac{d\theta_0}{dz} + K\left[\frac{\partial^2 \theta}{\partial x^2} + \frac{\partial^2 \theta}{\partial z^2}\right] \tag{5}$$

where the prognostic variables (u, v, w, θ) are perturbations from a basic state which is motionless, hydrostatic, and horizontally homogeneous with a constant stability (basic state quantities are denoted by subscript zero); σ_x and σ_z are the Rayleigh friction coefficients of horizontal and vertical momentum, while K is the eddy exchange coefficient for heat: these are considered as constants in the specific experiments in this study. The parameter λ is used to trace the nonhydrostatic effects. As evident in (3), $\lambda = 1$ and $\lambda = 0$ refer to nonhydrostatic and to hydrostatic sets of equations, respectively.

The procedure to derive the analytic solution of Defant's model was discussed in detail in Pielke (1984) and Martin (1981). For the purpose of this study, only the final solution set is listed here:

$$\begin{aligned} u(x, z, t) &= \tilde{u}(z)e^{i\omega t}\cos kx \\ v(x, z, t) &= \tilde{v}(z)e^{i\omega t}\cos kx \\ w(x, z, t) &= \tilde{w}(z)e^{i\omega t}\sin kx \\ p(x, z, t) &= \tilde{p}(z)e^{i\omega t}\sin kx \\ \theta(x, z, t) &= \tilde{\theta}(z)e^{i\omega t}\sin kx \end{aligned}$$

$$k = \frac{2\pi}{L_x}, \quad \omega = \frac{2\pi}{P}, \quad i = \sqrt{-1} \tag{6}$$

where k, L_x are horizontal wavenumber and wavelength, ω, P are the frequency and period of the heating function, and

$$\tilde{u}(z) = -\frac{1}{k} \cdot \frac{rM}{b^2 - a^2} \cdot (ae^{az} + be^{-bz})$$

$$\tilde{v}(z) = \frac{f}{i\omega + \sigma_x} \frac{1}{k} \frac{rM}{b^2 - a^2} (ae^{az} + be^{-bz})$$

$$\tilde{w}(z) = \frac{-rM}{b^2 - a^2}(e^{az} - e^{-bz})$$

$$\tilde{p}(z) = -\frac{Mg}{\theta_0\alpha_0}\frac{1}{b^2 - a^2}(ae^{az} + be^{-bz})$$

$$\tilde{\theta}(z) = \frac{M}{b^2 - a^2}[(b^2 - s)e^{az} - (a^2 - s)e^{-bz}]. \quad (7)$$

The parameters a and b are obtained from:

$$a^2 = b^2 = \frac{\eta^2 + s}{2} \pm \frac{1}{2}[(\eta^2 - s)^2 + 4\epsilon r]^{1/2}$$

$$a = \pm\sqrt{a^2}, \quad b = \pm\sqrt{b^2}. \quad (8)$$

As in Martin and Pielke (1983), the negative root is used for a and the positive root for b; with

$$\eta^2 = \lambda k^2 \frac{(i\omega + \sigma_x)(i\omega + \sigma_z)}{(i\omega + \sigma_x)^2 + f^2}$$

$$r = -\frac{g}{\theta_0} k^2 \frac{i\omega + \sigma_x}{(i\omega + \sigma_x)^2 + f^2}$$

$$\epsilon = \beta/K \quad \left(\beta = \frac{d\theta_0}{dz}\right)$$

$$s = \frac{i\omega}{K} + k^2. \quad (9)$$

As can be seen from above, when the hydrostatic assumption is made, $\lambda = 0$, thus $\eta^2 = 0$, and a and b are obtained from

$$a_H^2 = b_H^2 = \frac{s}{2} \pm \frac{1}{2}(s^2 + 4\epsilon r)^{1/2}$$

$$a_H = \pm\sqrt{a_H^2}, \quad b_H = \pm\sqrt{b_H^2} \quad (10)$$

where the subscript H of any quantity denotes hydrostatic, and the a_H and b_H are obtained in the same manner as a and b.

Since all the prognostic variables are functions of a and b, we know that they will have different solutions if a_H and b_H replace a and b. Thus, to obtain the exact solution for the differences between the hydrostatic and nonhydrostatic quantities, we need to consider this difference in all the prognostic variables in the governing equations.

The residual (i.e., nonhydrostatic) pressure perturbation (denoted as R, where $R \equiv p - p_H$) is obtained as follows:

$$\text{Take } \frac{\partial}{\partial x}(1): \quad \frac{\partial^2 p}{\partial x^2} = -\frac{1}{\alpha_0}\frac{\partial}{\partial x}\frac{\partial u}{\partial t} + \frac{f}{\alpha_0}\frac{\partial v}{\partial x} - \frac{\sigma_x}{\alpha_0}\frac{\partial u}{\partial x} \quad (11)$$

$$\text{Take } \frac{\partial}{\partial z}(3): \quad \frac{\partial^2 p}{\partial z^2} = -\frac{1}{\alpha_0}\frac{\partial}{\partial z}\frac{\partial w}{\partial t} + \frac{g}{\theta_0\alpha_0}\frac{\partial \theta}{\partial z} - \frac{\sigma_z \partial w}{\alpha_0 \partial z}. \quad (12)$$

Similarly for the hydrostatic system, we obtain

$$\frac{\partial^2 p_H}{\partial x^2} = -\frac{1}{\alpha_0}\frac{\partial}{\partial x}\frac{\partial u_H}{\partial t} + \frac{f}{\alpha_0}\frac{\partial v_H}{\partial x} - \frac{\sigma_x}{\alpha_0}\frac{\partial u_H}{\partial x} \quad (13)$$

$$\frac{\partial^2 p_H}{\partial z^2} = \frac{g}{\theta_0\alpha_0}\frac{\partial \theta_H}{\partial z}. \quad (14)$$

Subtracting (13) from (11), and (14) from (12), and adding the results yields the Poisson equation for the pressure residual term:

$$\nabla^2 R = -\frac{1}{\alpha_0}\frac{\partial}{\partial x}\frac{\partial}{\partial t}(u - u_H) + \frac{f}{\alpha_0}\frac{\partial}{\partial x}(v - v_H) - \frac{\sigma_x}{\alpha_0}\frac{\partial}{\partial x}(u - u_H) + \frac{g}{\theta_0\alpha_0}\frac{\partial}{\partial z}(\theta - \theta_H) - \frac{1}{\alpha_0}\frac{\partial}{\partial z}\frac{\partial w}{\partial t} - \frac{\sigma_z}{\alpha_0}\frac{\partial w}{\partial z}. \quad (15)$$

Using Defant's analytic solutions, listed in Eq. (7), we have, for example, the first right-hand side term above:

$$-\frac{1}{\alpha_0}\frac{\partial}{\partial x}\frac{\partial}{\partial t}(u - u_H) = \frac{i\omega rM}{\alpha_0}e^{i\omega t} \times \sin kx\left[\frac{a_H e^{a_H z} + b_H e^{-b_H z}}{b_H^2 - a_H^2} - \frac{ae^{az} + be^{-bz}}{b^2 - a^2}\right].$$

Similar expressions can be obtained for all other terms on the right-hand side of Eq. (15). After rearrangements, the Poisson equation for the pressure residual can be rewritten as:

$$\nabla^2 R = \frac{M}{\alpha_0}e^{i\omega t}\sin kx[Ae^{az} + Be^{-bz} + Ce^{a_H z} + De^{-b_H z}] \quad (16)$$

where

$$\left.\begin{aligned} A &= \frac{a}{b^2 - a^2}\left[\frac{-rf^2}{i\omega + \sigma_x} - r\sigma_x + r\sigma_z + \frac{g}{\theta_0}(b^2 - s)\right] \\ B &= \frac{b}{b^2 - a^2}\left[\frac{-rf^2}{i\omega + \sigma_x} - r\sigma_x + r\sigma_z + \frac{g}{\theta_0}(a^2 - s)\right] \\ C &= \frac{a_H}{b_H^2 - a_H^2} \times \left[i\omega r + \frac{rf^2}{iw + \sigma_x} + r\sigma_x - \frac{g}{\theta_0}(b_H^2 - s)\right] \\ D &= \frac{b_H}{b_H^2 - a_H^2} \times \left[i\omega r + \frac{rf^2}{i\omega + \sigma_x} + r\sigma_x - \frac{g}{\theta_0}(a_H^2 - s)\right] \end{aligned}\right\}. \quad (17)$$

Equations (16) and (17) provide the exact solution for the pressure residual term which represents the analytic difference of pressure perturbation between hydrostatic and nonhydrostatic states in Defant's model. The formulation, however, has quantities belonging to both states (the a, b, and a_H, b_H) which need to be evaluated simultaneously. This means that the complete residual can only be used for diagnostic purposes if applied in a nonlinear numerical model since it would be just as easy to use the complete anelastic equation for p [i.e., the nonlinear analog to the sum of (11) and (12)].

In order to obtain a practical method which calculates nonhydrostatic effects using only information available from a hydrostatic model following Pielke (1972), the equation for the quasi-nonhydrostatic residual (denoted as R_H) is obtained in the same manner as in Eqs. (11)–(15), except that the difference between hydrostatic and nonhydrostatic appears only in the time derivative term and the vertical friction term. Thus, we have

$$\nabla^2 R_H = -\frac{1}{\alpha_0}\frac{\partial}{\partial x}\frac{\partial u}{\partial t} + \frac{1}{\alpha_0}\frac{\partial}{\partial x}\frac{\partial u_H}{\partial t} - \frac{1}{\alpha_0}\frac{\partial}{\partial z}\frac{\partial w}{\partial t} - \frac{\sigma_z}{\alpha_0}\frac{\partial w}{\partial z}.$$

Using the incompressible continuity, the above equation is reduced to

$$\nabla^2 R_H = \frac{1}{\alpha_0}\frac{\partial}{\partial x}\frac{\partial u_H}{\partial t} - \frac{\sigma_z}{\alpha_0}\frac{\partial w}{\partial z}. \tag{18}$$

This is analogous to the form as applied in Pielke (1972), and Martin and Pielke (1983) in their numerical model evaluations.

Comparing (18) with (15), we see that (18) can be obtained directly from (15) by neglecting the differences between u, v, θ and u_H, v_H, θ_H, respectively, and considering incompressibility. Using the incompressibility, Eq. (18) becomes

$$\nabla^2 R_H = \frac{1}{\alpha_0}\frac{\partial}{\partial x}\frac{\partial u_H}{\partial t} + \frac{\sigma_z}{\alpha_0}\frac{\partial u_H}{\partial x}. \tag{19}$$

It is then clear that (19) is of practical value because only hydrostatic quantities are involved in the estimation of the nonhydrostatic effects, all of which can be obtained in a hydrostatic model. Also, comparing (19) with (15), we see that the neglected terms in deriving (19) are the first four terms in (15), which involve the immediate feedbacks associated with the buoyancy, horizontal friction, and the Coriolis terms.

In terms of Defant's analytic solutions, Eq. (19) is written as

$$\nabla^2 R_H = \frac{M}{\alpha_0} e^{i\omega t} \sin kx [C' e^{a_H z} + D' e^{-b_H z}] \tag{20}$$

where

$$C' = \frac{a_H}{b_H^2 - a_H^2}(i\omega r + r\sigma_z)$$

$$D' = \frac{b_H}{b_H^2 - a_H^2}(i\omega r + r\sigma_z).$$

The solutions for Eqs. (16) and (20) are obtained using the method of separation of variables. However, it is straightforward to show that the solution for R_H is exactly the solution for R except that a_H and b_H replace a and b. Written formally, the solution for R is

$$R = \frac{M}{\alpha_0} e^{i\omega t} \sin kx \left[\frac{A}{a^2 - k^2} e^{az} + \frac{B}{b^2 - k^2} e^{-bz} + \frac{C}{a_H^2 - k^2} e^{a_H z} + \frac{D}{b_H^2 - k^2} e^{-b_H z}\right] \tag{21}$$

with A, B, C, D defined in Eq. (17).

In the next section, the pressure terms (p, p_H) and the residual terms (R, R_H) will be analyzed as functions of the horizontal length scale, large scale stability, subgrid-scale heat diffusion, heating amplitude and surface friction. The purpose of these analyses is to determine how the nonhydrostatic pressure residual varies with changing physical conditions within the framework of Defant's model. Furthermore, as stated before, since the nonhydrostatic effects are evaluated using Eqs. (16) and (17), rather than using $\lambda = 1$ in Defant's model, it seems necessary to show the consistency of the results obtained from the two independent procedures. Unless otherwise mentioned, the values of the parameters used for the examples are those listed in Table 1.

3. Analyses of the residuals

Figure 1 shows the maximum amplitude for the pressure terms (p, p_H) and the residual terms (R, R_H) as functions of horizontal length scale (L) plotted on a logarithmic scale. (All the dependent variables in the following section and figures are presented at their maximum.) The range of scales is chosen from 200 m to 50 km, which should cover most of the spatial scales

TABLE 1. Control values for the parameters.

$\beta\left(=\frac{d\theta_0}{dz}\right)$	0.01°C km^{-1}
K	10 m^2 s^{-1}
α_0	0.758 (m^3 kg^{-1})
σ_x, σ_z	10^{-3} (s^{-1})
P	1 h
θ_0	273 K
M	10°C
L	1 km
z	15 m
f	10^{-4} (s^{-1})

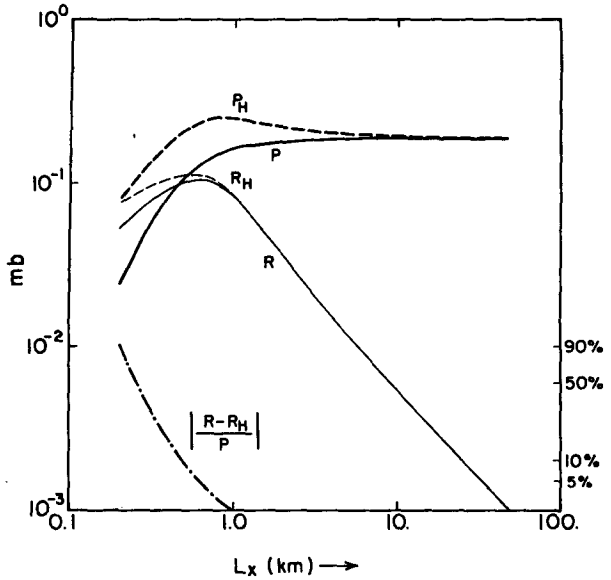

FIG. 1. Variations of the pressure perturbation and the residual terms (p, p_H, and R, R_H; mb), and the absolute error term ($|R - R_H|/|P|$; %), as a function of the horizontal length scale (L_x). Other physical parameters are given in Table 1.

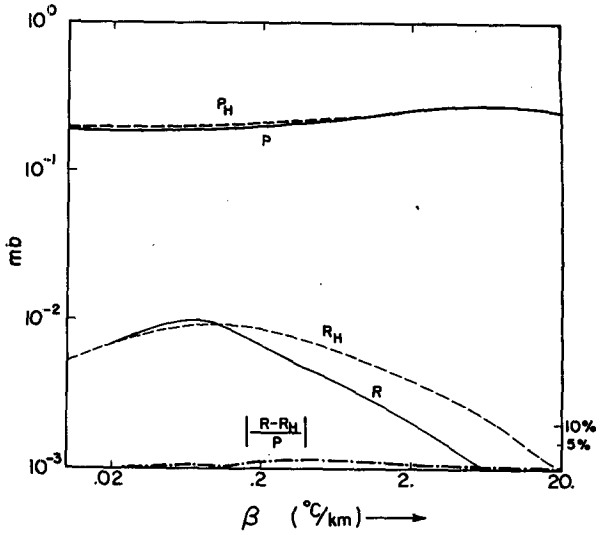

FIG. 2. As in Fig. 1 except as a function of the stability parameter (β). L_x = 10 km.

in which there is concern regarding the adequacy of the hydrostatic assumption in a model. Since the pressure perturbations are caused by surface heating in this study, and since all perturbation quantities decrease exponentially with height, the perturbations are evaluated near the surface (z = 15 m). All the pressure and the residual terms are given in units of millibar.

As can be seen, when the length scale becomes large, p becomes nearly constant. The difference between p and p_H (i.e., R) becomes negligible for larger scales. This feature can be explained using Eq. (9): as $L \to \infty$, $k \to 0$, and $\eta^2 \to 0$, $r \to 0$; also $s = s(\omega, k)$. Thus, there is a decreasing dependence on the length scale as it becomes large, resulting in a nearly constant p. Also, it can be seen that there are virtually no differences between a, b and a_H, b_H, respectively, when the scale is large.

For smaller scales, k^2 becomes large and the situation is more complicated. From Fig. 1, we see that for scales less than about 1 km, the residuals are of the same order of magnitude as the pressure terms. This indicates that for such small scales, the nonhydrostatic effect is significant, and that p_H is significantly overestimating the true pressure perturbation. Pielke (1972, Fig. 19) schematically illustrated how the hydrostatic pressure overestimates the real pressure.

What is also of interest here is how R_H behaves as compared with R. From Fig. 1 we see that for length scales larger than about 1 km, there is essentially no difference between R and R_H, while for the smaller scales this difference becomes significant. The quantity $|(R - R_H)/P|$, hereafter called the absolute error and expressed as a percentage, is also plotted. This measure illustrates how much error is introduced as a fraction of the true pressure perturbation, when R_H is used instead of the complete nonhydrostatic pressure residual, R. Figure 1 shows that this absolute error drops to essentially zero for $L > 1$ km, but increases sharply when $L < 1$ km. It is clear that under this near-neutral condition (β = 0.01°C km^{-1}) with a surface heating of 10°C effective for one hour, the quasi-nonhydrostatic residual method gives an accurate measure of the nonhydrostatic effect for horizontal length scales as small as about 1 km.

The dependence of p, p_H, R and R_H on the large-scale stability is illustrated for L = 10 km (Fig. 2) and L = 1 km (Fig. 3). The strength of the surface heating,

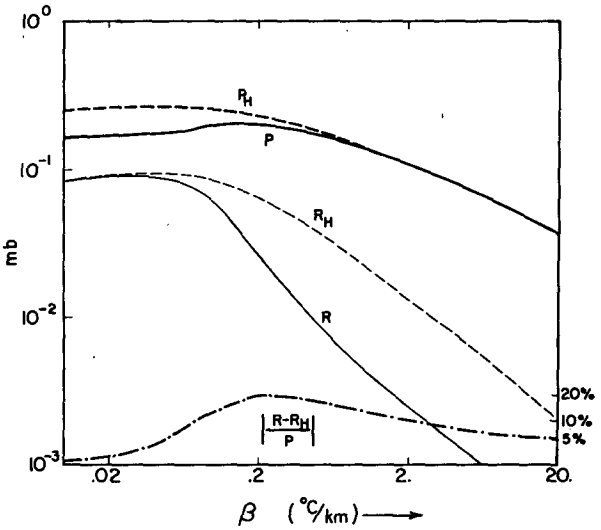

FIG. 3. As in Fig. 2 with L_x = 1 km.

the heating period, and the strength of the eddy heat diffusion are all the same as used to create Fig. 1. In Fig. 2, we see that for $L = 10$ km, the difference between p and p_H is negligible for all the chosen stabilities (β: from 0.01 to 20°C km^{-1}). The R_H and R, although they differ somewhat relative to one another, are both negligibly small compared with the pressure terms. Thus, the absolute error term is very small for all the chosen stabilities (the largest error is 1.5 percent, occurring at $\beta = 0.4$°C km^{-1}). The result shown here indicates that for the scales normally considered in mesoscale analyses ($L = 10$ km or larger), in which the driving mechanism is surface heating and the upward transport of this heating is primarily through the associated turbulent eddy processes, the situation is approximately hydrostatic and the residual method can be used to accurately calculate the small nonhydrostatic effects.

When the length scale is reduced to 1 km, however, the residuals become relatively larger than for the previous case and, as seen in Fig. 3, R_H departs significantly from R for a wide range of stabilities. From Fig. 3, we see that for the less stable situations ($\beta \leq 0.1$°C km^{-1}), the residual is on the same order of magnitude as the true pressure perturbation, while for the strongly stable situations ($\beta \geq 0.1$°C km^{-1}) R_H differs more significantly from R. The physical mechanisms which contribute to this discrepancy will be discussed in more detail in the next section.

The dependence of the pressure and the residual terms upon the strength of the eddy heat diffusion is shown in Fig. 4. The horizontal length scale is 1 km, and the other parameters are the same as in the above cases. The range of the (constant) diffusion coefficient

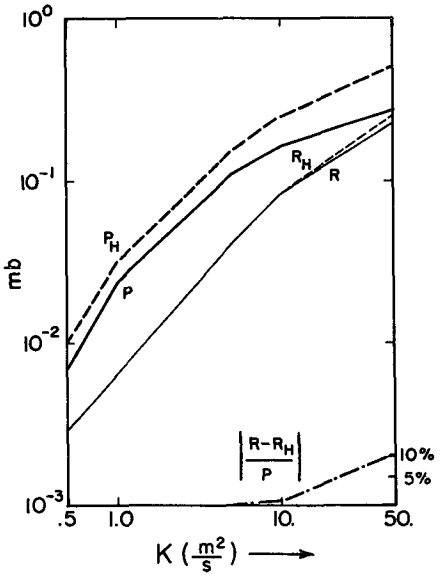

FIG. 4. As in Fig. 1 except as a function of the heat diffusion coefficient (K).

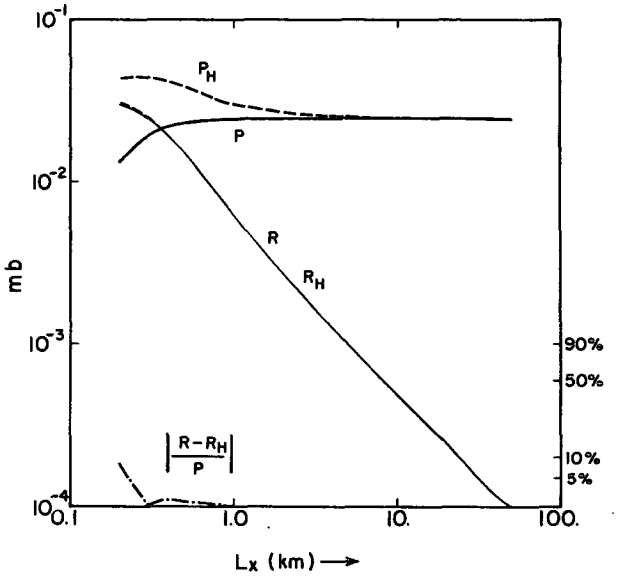

FIG. 5. As in Fig. 1 except $K = 1.0$ (m^2 s^{-1}).

K is from 0.5 to 50 (m^2 s^{-1}). It is seen in Fig. 4 that as the strength of eddy heat diffusion increases, the pressure perturbations increase. The hydrostatic pressure perturbation consistently exceeds the real pressure perturbation. For this small horizontal scale (1 km), the residual is the same order of magnitude as the pressure terms. Here R_H gives a very accurate measure of the nonhydrostatic effect due to the heat diffusion process, except when the diffusion coefficient becomes very large.

Figures 5 and 6 show the dependence of P, P_H, R, and R_H on the horizontal scale of heating for small K

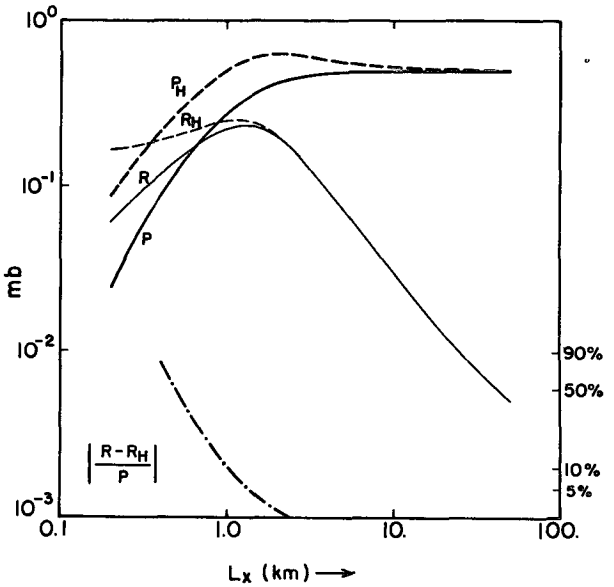

FIG. 6. As in Fig. 1 except $K = 50$ (m^2 s^{-1}).

($K = 1$ m^2 s^{-1}) and large K ($K = 50$ m^2 s^{-1}), respectively. In Fig. 5 we see that when the eddy heat diffusion is sufficiently small, R_H gives an accurate measure of the nonhydrostatic effects for scales as small as about 300 m. For very large diffusion (Fig. 6), the residual is the same order of magnitude as the pressure for scales of a few kilometers or less. The absolute error is rather large for the small scales, and drops to essentially zero at scales greater than about 3 km. The increase of the nonhydrostatic effect with increasing strength of the eddy heat diffusion was also illustrated in Martin and Pielke (1983).

The discrepancy between R and R_H for very large K (Fig. 4) is found only for small horizontal scales. Figure 6 shows that for the same strength of heat diffusion ($K = 50$ m^2 s^{-1}), the difference between R and R_H is essentially zero at scales larger than about 3 km. This implies that when a strong energy input is coupled with a small horizontal scale, there may be buoyancy oscillations excited which cause departures of R_H from R. From Figs. 5 and 6 we see that either increasing the horizontal scale or decreasing the strength of heat diffusion will minimize the discrepancy between R_H and R.

The strength of the surface heating is obviously important in producing nonhydrostatic effects. However, this forcing appears only as a constant in Defant's linear model [i.e., see Eq. (7) for $\tilde{\theta}(z)$], thus not allowing the interactions between surface heating and mesoscale circulations to take place. Martin and Pielke (1983) discussed in more detail the effect of surface heating using a nonlinear model.

Finally, the effect of the frictional term on pressure and the residual terms is shown in Fig. 7. The physical parameters are the same as in Fig. 1 except that the (constant) frictional coefficient is reduced by one order of magnitude. Comparing Fig. 7 with Fig. 1, we see that reducing the friction produces negligible effects upon the pressure perturbations. The absolute error is within 2 percent for scales larger than about 2 km.

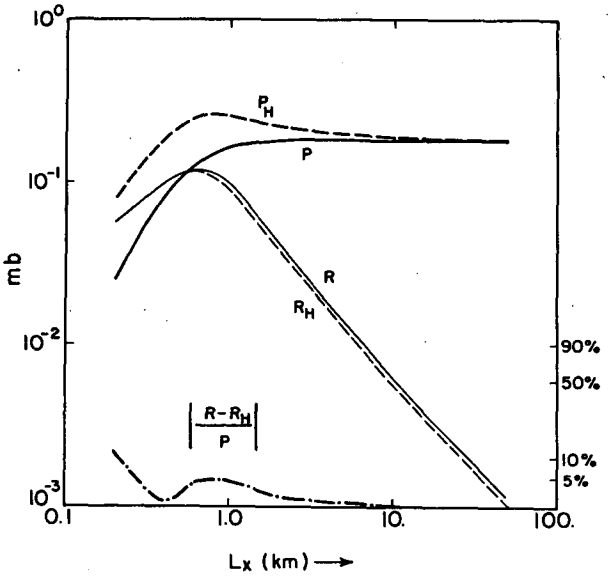

FIG. 7. As in Fig. 1 except with a smaller Rayleigh friction coefficient (10^{-4} s^{-1}).

4. Comparison of residual methodologies

For the purpose of comparing the approach discussed in Section 3 for the evaluation of the nonhydrostatic residual, two other different approximate residual formations (based on the Defant model) are analyzed in this section. Also presented is a discussion of the physical mechanisms which contribute to the discrepancies between the approximate residuals as compared with the exact residual.

Using Defant's linear model, the Orlanski (1981) pressure correction term is derived from a vertical integration of the local time derivative of the hydrostatically-obtained vertical velocity. Written in an appropriate form for the comparisons here, the equation for the Orlanski residual (hereafter denoted to as R_Q) is

$$\frac{\partial^2}{\partial z^2} R_Q = -\frac{1}{\alpha_0} \frac{\partial}{\partial z} \frac{\partial w_H}{\partial t}. \tag{22}$$

It is seen from Eqs. (15), (18), and (22) that R_Q can be derived from (15) by making, in addition to the simplifications made for obtaining R_H, two simplifications concerning the horizontal second-derivative of the residual and the vertical friction term. This can be clearly seen if we compare the formal solutions for R_H and R_Q;

$$R_H = \frac{1}{\alpha_0} e^{i\omega t} \sin kx \left(\frac{rM}{b_H^2 - a_H^2}\right) \times \left[(i\omega)\left(\frac{a_H}{a_H^2 - k^2} e^{a_H z} + \frac{b_H}{b_H^2 - k^2} e^{-b_H z}\right) + \sigma_z \left(\frac{a_H}{a_H^2 - k^2} e^{a_H z} + \frac{b_H}{b_H^2 - k^2} e^{-b_H z}\right)\right], \tag{23}$$

$$R_Q = \frac{1}{\alpha_0} e^{i\omega t} \sin kx \left(\frac{rM}{b_H^2 - a_H^2}\right) \times \left[(i\omega)\left(\frac{1}{a_H} e^{a_H z} + \frac{1}{b_H} e^{-b_H z}\right)\right]. \tag{24}$$

Neglecting the friction term, we see that R_Q can be obtained directly from R_H by setting k to zero. Thus when the horizontal scale of heating becomes large, in the absence of friction (which as discussed in the last section is a relatively small term), R_Q and R_H are asymptotic to the same value.

Mathematically, the quantity k^2 is associated with the x-direction second-derivative of the residual, which is derived from the horizontal equation of motion in

which the nonhydrostatic effect is explicitly included. That is, from Eq. (1) we have

$$\frac{\partial^2}{\partial x^2}(p - p_H) = -\frac{1}{\alpha_0}\frac{\partial}{\partial t}\frac{\partial}{\partial x}(u - u_H) + \frac{f}{\alpha_0}\frac{\partial}{\partial x}(u - u_H) - \frac{\sigma_x}{\alpha_0}\frac{\partial}{\partial x}(u - u_H). \quad (25)$$

Therefore, setting k^2 to zero is also equivalent to neglecting the nonhydrostatic horizontal momentum residual (i.e., the horizontal velocity residual).

Since in an incompressible system the horizontal velocity gradient is directly related to the generation of vertical acceleration, it is thought necessary to further examine the effect of neglecting k^2 (but retaining other important terms). For this purpose, a new residual (hereafter denoted as R_z) is considered which is obtained from the complete vertical equation of motion; i.e.,

$$\frac{\partial^2}{\partial z^2}R_z = -\frac{1}{\alpha_0}\frac{\partial}{\partial z}\left(\frac{\partial w_H}{\partial t}\right) - \frac{\sigma_z}{\alpha_0}\frac{\partial w}{\partial z} + \frac{g}{\theta_0\alpha_0}\frac{\partial}{\partial z}(\theta - \theta_H). \quad (26)$$

Thus, there are four different residuals to be compared: R, R_H, R_Q, R_z, obtained from Eqs. (15), (18), (22), and (26), respectively. Aside from the friction and the Coriolis terms (which are found not essential to our main conclusion), R_H and R_Q differ from R and R_z in that the former do not include the nonhydrostatic buoyancy residual [i.e., the potential temperature residual term, as in Eqs. (15) and (26)]. On the other hand, R_z and R_Q differ from R and R_H in that the former neglect the nonhydrostatic horizontal momentum residual, or, equivalently, *they are based on the assumption of an infinite horizontal length scale.*

In order to have consistent numerical experiments with those in the previous section, the following computations are performed using, unless otherwise mentioned, the physical parameters listed in Table 1. Another set of experiments was also performed using the heating period of 12 hours. Since the general patterns of the residuals are similar using either 1 or 12 h as the heating period, only the results of using 1 h are analyzed here.

In Fig. 8, the four residuals are plotted as functions of the horizontal length scale for three selected stabilities. The magnitude of the total pressure perturbations are, for the scale range between about 1 and 10 km, on the order of 10^{-1} mb. We first see that for a given length scale, the nonhydrostatic residuals increase with decreasing stability. For the stable situation ($\beta = 10°C$ km^{-1}), all the residuals are about two orders of magnitude smaller than the total pressure perturbation; while for the near-neutral situation ($\beta = 0.1°C$ km^{-1}),

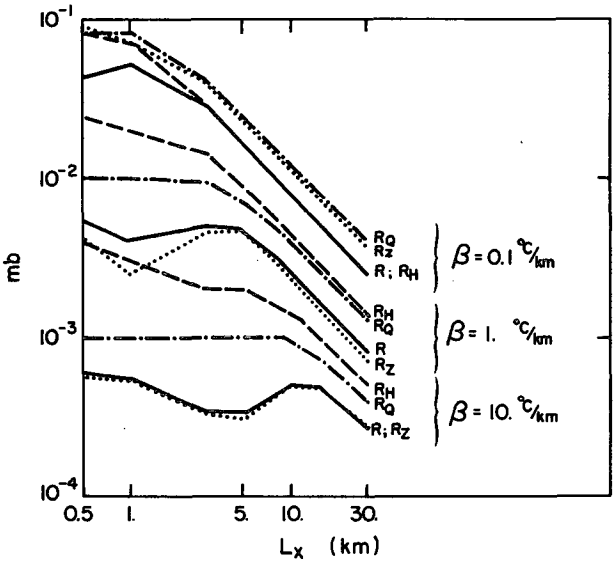

FIG. 8. The magnitudes (in mb) of the four residuals at $z = 15$ m: R (solid), R_H (dashed), R_z (dotted), and R_Q (dash-dot), as functions of the length scale and of three selected stabilities ($\beta = 0.1$, 1, 10°C km^{-1}, as shown).

the residuals are comparable to the total pressure perturbation for the smaller length scales. For a given stability, the residuals are generally decreasing with increasing length scale. The closer to the neutral state, the larger the rate of decrease of the residuals with increasing length scale. An exception to this is the nonmonotonic variation of R and R_z in the more stable categories which indicates that an optimal horizontal scale exists in which vertical acceleration is maximized as a result of contributions to convergence from opposite coasts (e.g., Abe and Yoshida, 1982). This relative maximum is not as significant in the 12-hour period experiments.

With regard to the comparison among the residuals, we see from Fig. 8 that in the stable situation, R_z matches with R, while R_H and R_Q deviate from R. On the other hand, in the near-neutral situation, R_H matches with R, while R_Q and R_z deviate from R. In order to more clearly analyze the relative magnitudes of the residuals, vertical profiles of the residuals are plotted for a selected length scale (1 km) and for two stabilities: $\beta = 0.001°C$ km^{-1} (Fig. 9), and $\beta = 10°C$ km^{-1} (Fig. 10). The magnitudes of the corresponding total pressure perturbations are also shown to indicate the possible absolute errors which are introduced when a certain residual is used.

From Fig. 9 we see that in the near-neutral situation, R_H matches with R everywhere, while R_z and R_Q are both about two orders of magnitude larger than R. Furthermore, both R_z and R_Q are about more than one order of magnitude larger than the total pressure perturbation. It seems clear that the R_Q-approach should

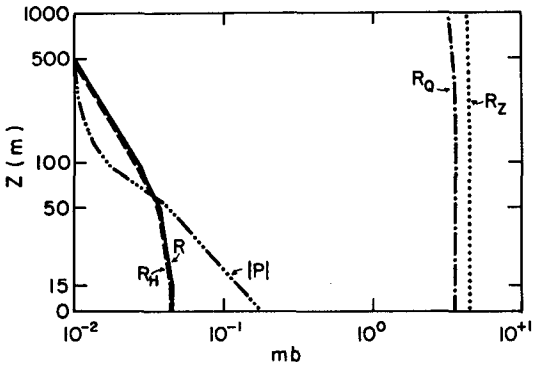

FIG. 9. Vertical profiles of the four residuals (notations are the same as those in Fig. 8) and $|p|$ for the near-neutral stability case (β = 0.001°C km^{-1}). The vertical levels are at z = 0, 15, 50, 100, 500 and 1000 (m).

not be considered for the situations where the environmental stability is near neutral. On the other hand, R_H provides an accurate measure of the nonhydrostatic effect under the near-neutral condition.

From Fig. 10, we see that in the stable situation, R_z matches with R while R_Q and R_H deviate somewhat from R, with R_Q slightly better than R_H. In this case, however, all the residuals are almost more than two orders of magnitude smaller than the total pressure perturbation. Clearly this result indicates that nonhydrostatic effects are negligible in the stable situation, and therefore the discrepancies are of little practical importance.

As discussed previously, the difference between the exact residual and other residuals is related to the nonhydrostatic buoyancy and horizontal momentum residuals. That is, the horizontal momentum change and the buoyancy associated with the surface heating are the two most important physical mechanisms which contribute to the generation of nonhydrostatic effects, for the situations considered in this study. The vertical profiles of θ and θ_H (Fig. 11), and u and u_H (Fig. 12), are plotted for the same length scale (1 km) and the same stabilities (β = 0.001; 10°C km^{-1}). From Fig. 11 we see that θ is slightly larger than $\theta_H(\theta - \theta_H \leqslant 0.1°C)$ for the stable situation, while they match with each other everywhere in the near-neutral situation. This explains why R_Q and R_H (in which the $(\theta - \theta_H)$ term is neglected) deviate from R for the stable situation. Physically, this implies that for a system being heated from below, the more thermodynamically stable the system, the larger the fractional contribution of the nonhydrostatic buoyancy to the residual that is generated within the system. In the absolute sense, however, the nonhydrostatic effect is negligible in this case as compared with the total pressure perturbation.

From Fig. 12, we see that for the stable situation u and u_H are almost equal, while for the near-neutral situation they differ significantly from each other. Again, this explains why R_Q and R_z [in which the $(u - u_H)$ term is neglected] deviate significantly from R in the near-neutral case, and R_H [which contains the $(u - u_H)$ term] matches with R. Physically, this implies that for an incompressible system, the closer the system's stability is toward neutral stratification, the stronger is its velocity perturbation generated within the system, and therefore the horizontal momentum change plays a more important role in generating nonhydrostatic effects (i.e., vertical acceleration) as compared with the situation where there are only weak horizontal velocity perturbations.

Finally, computations presented in Figs. 8–12 were repeated for various β values between those of the very stable case (β = 10°C km^{-1}) and the almost neutral case (β = 0.001°C km^{-1}). These results, which are not shown, reflected intermediate features to those presented in those figures.

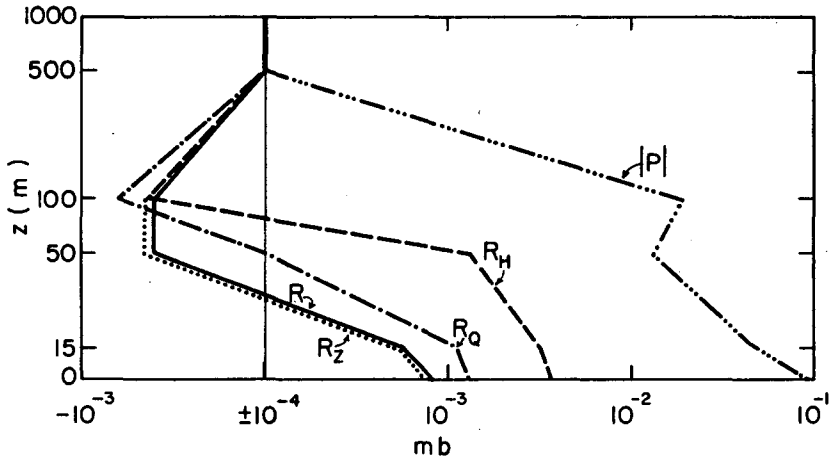

FIG. 10. As in Fig. 9 except for β = 10°C km^{-1}.

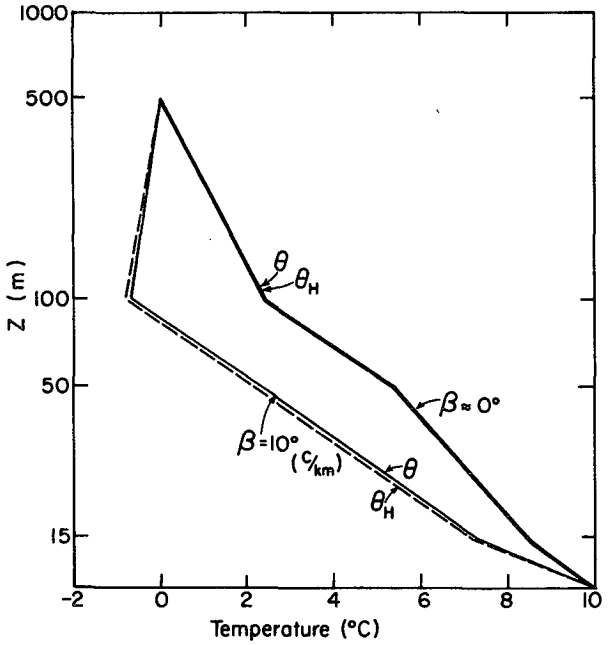

FIG. 11. Vertical profiles of θ (solid) and θ_H (dashed) for the near-neutral case (thick line) and the stable case (thin line).

5. Conclusion

Defant's linear model is used to derive a mathematically exact solution for the nonhydrostatic pressure residual (total pressure perturbation minus hydrostatic pressure perturbation). From the complete form of this exact residual we can see that the thermally-induced nonhydrostatic effects are caused, within the linear framework, by physical processes such as horizontal momentum variations, buoyancy effects, frictional effects, and Coriolis effects. Since the complete residual requires both hydrostatic and nonhydrostatic quantities to be evaluated simultaneously, this residual can only be used in a diagnostic analysis for numerical modeling purposes. For the purposes of deriving a prognostic approach to incorporate nonhydrostatic effects into one or more subdomains of a mesoscale model, the complete residual must be simplified so as to neglect those terms which cannot be evaluated without a complete nonhydrostatic model.

One type of simplification made to the exact residual for the purpose of deriving a prognostic approach is to neglect the nonhydrostatic buoyancy residual term. Together with the incompressible continuity, this results in the residual approach introduced in Pielke (1972). Aside from the horizontal friction and the Coriolis terms (which are found not to be critical to the discussions of this study), the Pielke (1972) method differs from the exact residual only in the buoyancy residual term which, in the experiments performed in this study, is relatively important only in the very thermally stable environments. For such stable situations, the nonhydrostatic pressure perturbations are generally about two orders of magnitude smaller than the total pressure perturbation. Thus, the discrepancy between the approximate residual and the exact residual is of little practical importance.

For near-neutral stabilities, the Pielke (1972) residual approach has been found to be able to provide accurate approximations to the true pressure perturbation, indicating that it is of practical value for evaluating nonhydrostatic effects within a subdomain of a mesoscale model, when the environment is in a near-neutral state.

Another type of simplification is to neglect the nonhydrostatic horizontal momentum residual term. Within Defant's linear framework, this simplification results in the residual approach introduced in Orlanski (1981). It is found that this residual can be obtained from the exact residual by merely making an assumption that the involved horizontal length scale is very large (i.e., a wavenumber approaching zero). This simplification is equivalent to neglecting the nonhydrostatic velocity perturbation. In a near-neutral environment, it is found that the nonhydrostatic velocity (momentum) residual is relatively much more important than in a stable environment. Neglecting this velocity residual caused the Orlanski residual to overestimate the nonhydrostatic pressure perturbation by about two orders of magnitude.

Physically, the above results imply that for an incompressible system being heated from below, the actual pressure perturbation tends to depart from the hydrostatic pressure perturbation by an amount which depends primarily on the system's environmental thermal stability and horizontal scale of heating. For a sufficiently stable system, there are negligible nonhydrostatic effects. On the other hand, when the stability is near-neutral, relatively stronger perturbations will develop which tend to more closely connect the vertical acceleration with the horizontal momentum variations. In such situations, a residual approach must include the nonhydrostatic momentum residual term, such as the approach of Pielke (1972), in order to accurately evaluate the nonhydrostatic effects. The resid-

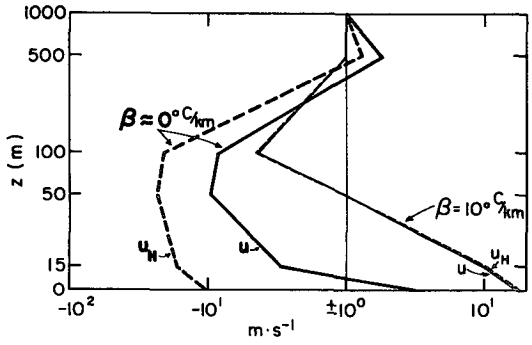

FIG. 12. Vertical profiles of u (solid) and u_H (dashed) for the near-neutral case (thick line) and the stable case (thin line).

ual approach presented here has the utility that it can be applied for subregions within a mesoscale model where vertical accelerations are large, while in the remainder of the model, the hydrostatic assumption can be applied. At the boundaries of the model subdomain the boundary condition $R_H = 0$ would be applied in the solution of the nonlinear form of (18).

Acknowledgments. This work has been performed under the National Science Foundation Grants ATM 8304042 and ATM-8414181. Computations performed in this study were made at NCAR (NCAR is supported by the NSF) and on the CSU CYBER 205 with partial support provided by the Control Data Corporation. The authors appreciate the helpful discussions with Drs. W. Schubert and M. DeMaria. Comments by anonymous reviewers were valuable in improving and clarifying aspects of the paper. We thank Mr. C. Martin for providing the original computer program of Defant's model. Sara Rumley and Liz Lambert are thanked for aiding in the manuscript preparation, and Judy Sorbie for drafting the figures.

REFERENCES

Abe, S., and T. Yoshida, 1982: The effect of the width of a peninsula on the sea breeze. *J. Meteor. Soc. Japan,* **60,** 1074–1084.

Cotton, W. R., and G. J. Tripoli, 1978: Cumulus convection in shear flow three-dimensional numerical experiments. *J. Atmos. Sci.,* **35,** 1503–1521.

Defant, F., 1951: Local winds. *Compendium of Meteorology,* Amer. Meteor. Soc., 655–672.

Klemp, J. B., and R. B. Wilhelmson, 1978: The simulation of three-dimensional convective storm dynamics. *J. Atmos. Sci.,* **35,** 1070–1096.

Martin, C., 1981: Numerical accuracy in a mesoscale meteorological model. M.S. thesis, Dept. of Environmental Sciences, University of Virginia, Charlottesville, 86 pp.

——, and R. A. Pielke, 1983: The adequacy of the hydrostatic assumption in sea breeze modeling over flat terrain. *J. Atmos. Sci.,* **40,** 1472–1481.

Neumann, J., and Y. Mahrer, 1971: A theoretical study of the land and sea breeze circulations. *J. Atmos. Sci.,* **28,** 532–542.

Ogura, Y., and J. G. Charney, 1961: A numerical model of thermal convection in the atmosphere. *Proc. Int. Symp. Numerical Weather Prediction,* Tokyo, Meteor. Soc. Japan, 431–450.

Orlanski, I., 1981: The quasi-hydrostatic approximation. *J. Atmos. Sci.,* **38,** 572–582.

Pielke, R. A., 1972: Comparison of a hydrostatic and an anelastic dry shallow primitive equation model. NOAA Tech. Memo. ERL OD-13, 47 pp.

——, 1984: *Mesoscale Meteorological Modeling.* Academic Press, 612 pp.

Schlesinger, R. E., 1978: A three-dimensional numerical model of an isolated thunderstorm: Part I. Comparative experiments for variable ambient wind shear. *J. Atmos. Sci.,* **35,** 690–713.

Tapp, M. C., and P. W. White, 1976: A non-hydrostatic mesoscale model. *Quart. J. Roy. Meteor. Soc.,* **102,** 277–296.